**BKM**

# Fatigue in High Strength Steel

A new approach to predict crack propagation behaviour

Thomas Cornelius Hansen

# Contents

# II Preface

This report has been prepared as one part of the thesis required to obtain the Ph.d. degree at the Technical University of Denmark. The report is the result of a research project carried out at the Department of Structural Engineering, under the supervision of Prof.dr.techn M.P.Nielsen.

The project has been financed by Statens Teknisk Videnskabelige Forskningsråd.

This report deals with fracture mechanics of high strength steel. The main subjects are crack propagation under fatigue loading and presentation and evalution of a newly developed theory, which is able to predict crack propagation under dynamic loading.

I would like to thank my supervisor for giving valuable inspiration and encouragement during the project.

Finally I express my gratitude to all other persons, who contributed to the completion of this report.

Lyngby, November 1996

Thomas Cornelius Hansen

# III Abstract

The main purpose of this paper is to present some tests with high strength steel. The paper is a follow-up of the work on fatigue and crack propagation [94.1]. It is the purpose to further evaluate the new theory of crack propagation by comparing it's results with test results. The advantage of the new theory is that crack propagation may be predicted on the basis of knowledge of well-known material parameters, contrary to the empirical formulas, the parameters of which must be determined by time consuming fatigue tests.

The paper is divided into four main parts:
 -Fracture toughness standard tests (chapter 2)
 -Fatigue tests (chapter 3)
 -Prediction of crack propagation using the new theory, and comparing the theory with test results (chapter 4)

The relation between the stress intensity factor $K_I$ and the critical stress intensity factor $K_{IC}$ is the main issue. Tests determining $K_{IC}$ as a function of $K_I$ have been performed. It is shown that $K_{IC}$ is not a constant, but clearly depends on $K_I$. The results are used to predict fatigue behaviour of high strength steel using the Energy Crack Propagation Formula (ECP).

# IV Resume

Hovedformålet med denne afhandling er at præsentere en forsøgsserie med højstyrke stål. Afhandlingen er en opfølgning af den tidligere afhandling 'fatigue and crack propagation' [94.1]. Det er formålet yderligere at eftervise den nyudviklede revnevækst-teori ved at sammenholde dens resultater med forsøg. Fordelen ved den nye teori er, at den er baseret på velkendte materialeparametre, ikke på empiriske konstanter udledt ved tidskrævende udmattelsesforsøg.

Afhandlingen er inddelt i fire hoveddele:
-Standardforsøg til bestemmelse af
 kritisk spændingsintensitets faktor (kap.2)
-Udmattelsesforsøg (kap.3)
-Beregning af revnevækst vha den ny teori og
 sammenligning af teori med forsøg (kap.4)

Hovedemnet i rapporten er fastlæggelse af sammenhængen mellem spændingsintensitets faktoren $K_I$ og den kritiske spændingsintensitets faktor $K_{IC}$. Der er udført forsøg der bestemmer $K_{IC}$ som funktion af $K_I$. Det er vist, at $K_{IC}$ ikke er konstant, men tydeligt afhængig af $K_I$. Resultaterne er benyttet til at forudsige udmattelses-forløbet i højstyrkestål ved at benytte Energi Revnevækst Formlen (ECP).

# V Notations

a                 Crack length

$a_p$'            Fracture zone length

$a_y$            Plastic zone length

$l_e$            Crack length correction

B                 Thickness

W                 Width, Elastic energy

L                 Length

H                 Height

D                 Diameter

N                 Number of cyclic load steps

da/dN            Crack growth rate

P                 Force

$P_{min}$         Minimum force

$P_{max}$         Maximum force

$\Delta P$        Force increment under dynamic load ($P_{max}$-$P_{min}$)

$P_{cr}$          Critical force

$\sigma$                 Stress

$f_u$                Ultimate stress

$f_y$                Yield stress

$f_t$                Tensile strength or true fracture strength

$K_I$                Stress intensity factor

$\Delta K_I$             Stress intensity factor increment under dynamic load ($K_{Imax}$-$K_{Imin}$)

$K_{IC}$            Critical stress intensity factor

$R$                Stress ratio ($\sigma_{min}/\sigma_{max} = K_{Imin}/K_{Imax}$)

$f$                Frequency

$C,m$           Empirical constants in Paris' equation

$c,n$            Empirical constants, Weibull size effect parameters

$M',n'$         Empirical constants, $K_{IC}$ - $K_I$ relation

# Chapter 1

## Introduction

The purpose of this report is to present some test results on fatigue of high strength steel. Fatigue crack propagation is a well-known phenomenon. Normally it is studied by using empirical formulas. However at the Department of Structural Engineering, Technical University of Denmark, an energy balance crack growth formula has recently been developed [90.1]. This formula can be used to predict crack propagation arising both from static load and from fatigue loading.

The formula has been evaluated in the case of fatigue loading by the author in an earlier report [94.1]. An important assumption is that fatigue crack propagation depends upon a varying critical stress intensity factor $K_{IC}$. Normaly it is assumed that $K_{IC}$ is a constant material parameter. In the earlier work [94.1] it was shown that $K_{IC}$ definitely is not constant, but varies with the value of the stress intensity factor $K_I$ during crack propagation.

In this report the relation between the stress intensity factor $K_I$ and the critical stress intensity factor $K_{IC}$ will be analysed in detail by further test results and calculations. This report can be considered as a follow-up of the earlier work done by the author [94.1].

In this report tests with a Swedish high strength steel, Hardox 400 ( see appendix A), is presented. Firstly some fracture toughness standard tests are presented. The purpose of these tests is to determine the relation between the actual value of $K_I$ under which the crack is initiated and the critical value $K_{IC}$. Secondly some fatigue crack propagation tests will be presented. The relation between $K_I$ and $K_{IC}$ will be used in some crack propagation calculations to predict the fatigue crack growth behaviour and the results will be compared with the results from the fatigue tests.

1

# Chapter 2

## Fracture toughness standard tests

## 2.1 Introduction

In this chapter the critical stress intensity factor standard test will be described and the test results presented. The purpose of these tests primarily is to determine the critical stress intensity factor $K_{IC}$ and secondly to determine the relation between the actual value of $K_I$ under which the crack is initiated and the final value of $K_{IC}$, as the final value depends upon the value of $K_I$ during initiation.

| (mm) | B | W | a | H | D |
|------|------|------|------|------|------|
| HA400 | 30 | 80 | 40 | 100 | 24.5 |

Table 2.1 *Dimensions of the $K_{IC}$ standard test specimens*

A number of 30 specimens were tested for Hardox 400 steel with the dimensions shown in table 2.1. The crack length **a** was initiated a little longer than shown in the table, which will be commented upon, when treating the test results. Furthermore 10 tests were performed on specimens with the dimensions shown in table 2.2. These tests were made to examine the thickness effect. The specimens are numbered with two digits. All the tests with small B (B=20) have a number which starts with the digit 4. The number of the tests with large B (B=30) starts with the digits 1,2 or 3.

| (mm) | B | W | a | H | D |
|------|------|------|------|------|------|
| HA400 | 20 | 47.5 | 22.5 | 60 | 12.5 |

Table 2.2 *Dimensions of the $K_{IC}$ standard test specimens*

## 2.2 Test results

The $K_{IC}$ standard tests were performed in a hydraulic 170 kN dynamic and static load machine. The test equipment and the test procedure are described in detail in **[94.1]**.

In the following, two P-COD (Load - Crack opening displacement) curves will be presented as illustrative examples, one representing the large specimens (B=30 mm) and one for the small specimens (B=20 mm).

The P-COD curves for Hardox 400 with B=30 mm showed very brittle fracture behaviour, and when the critical force $P_{cr}$ was reached, it was not possible to measure any continuation of the curve. Therefore in this case $P_{cr}$ was determined as the maximum load instead of using the E24 method (see **[94.1]**). In figure 2.1 a typical P-COD curve for Hardox 400 (B=30 mm) is shown.
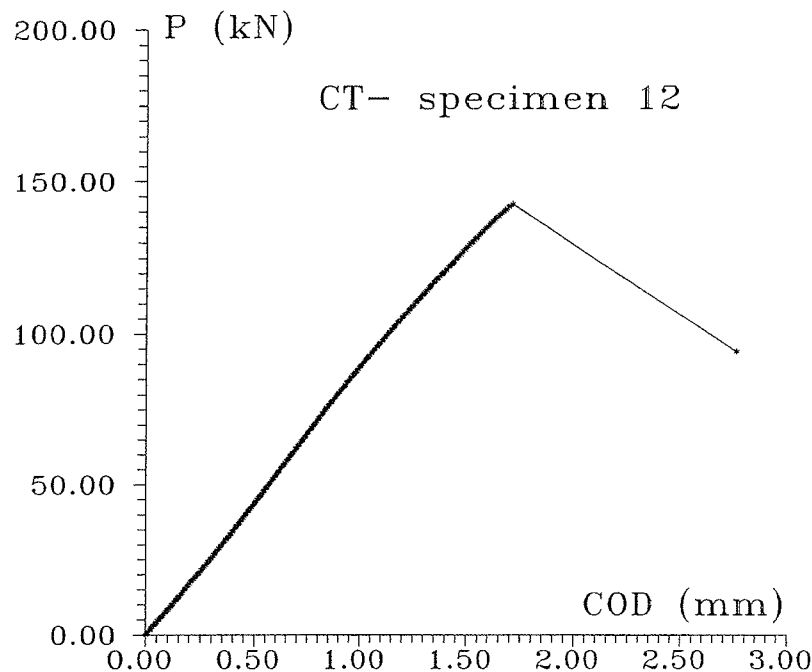


Figure 2.1 *P-COD curve for Hardox 400 (B=30 mm)*

In figure 2.2 a typical P-COD curve for Hardox 400 (B=20 mm) is shown. The curve follows the general type III curve (see [94.1]). The curve shows quite brittle behaviour and it was desided to determine the critical load as the maximum load to get similarity with the specimens B=30 mm.
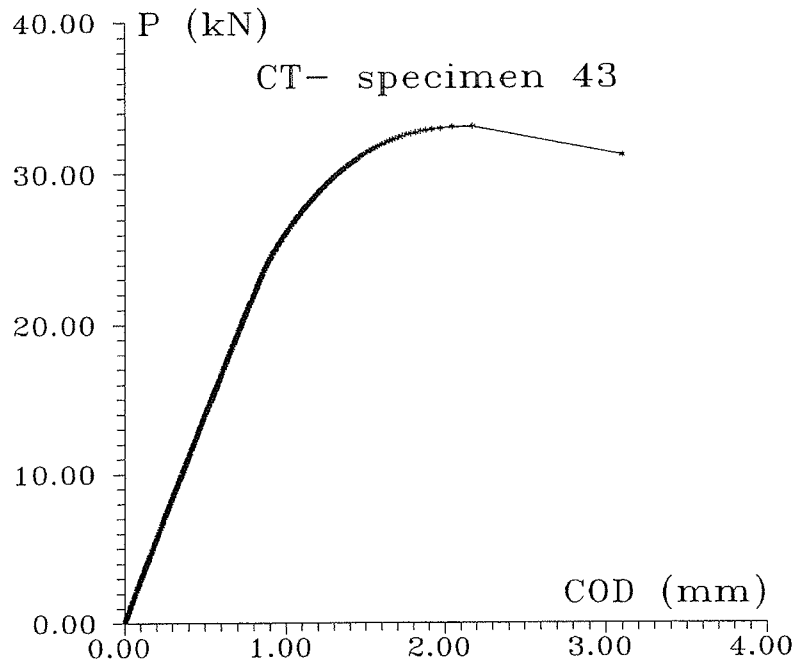


Figure 2.2 *P-COD curve for Hardox 400 (B=20 mm)*

The value of $P_{cr}$ for all the tests is listed in appendix C, together with the crack length **a**. The crack length **a** is measured after fracture, using the fact that the appearance of the fracture surface is very smooth in the area that has been cracked under cyclic loading and very rough in the area that has been fractured under static load. The crack length is measured as the length from the load application point to the transition point between the dynamic fracture area and the static fracture area. Figure 2.3 shows a broken CT-specimen. One might distinguish the two types of fracture areas.

4
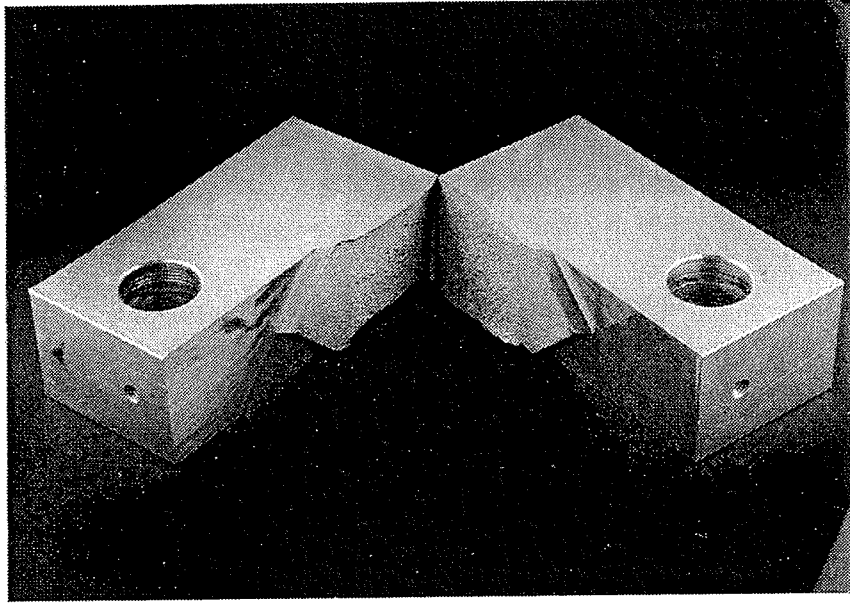
Figure 2.3 *Cracked CT-Specimen, showing the two typical fracture areas.*

The value of the crack length **a** is used to determine the critical stress intensity factor $K_{IC}$ and the value of $K_I$ under crack initiation. The stress intensity factor is determined by the formula, [86.1]:

$$K_I = \frac{P}{B \cdot W^{1/2}} \cdot \left( 29.6 \left(\frac{a}{W}\right)^{1/2} - 185.5 \left(\frac{a}{W}\right)^{3/2} \right.$$
$$\left. + 655.7 \left(\frac{a}{W}\right)^{5/2} - 1017 \left(\frac{a}{W}\right)^{7/2} + 638.9 \left(\frac{a}{W}\right)^{9/2} \right)$$

(2.1)

In this formulas $\Delta P = P_{max} - P_{min}$ is inserted instead of P when determining $\Delta K_I$ and $P = P_{cr}$ is inserted to determine $K_{IC}$. The minimum force is kept on a small value close to zero meaning $\Delta P \approx P_{max}$.

The measured values of a, $\Delta P$ and $P_{cr}$ and the calculated values of $K_I$ and $K_{IC}$ respectively are listed in appendix C.

5

## 2.3 Relation between $K_I$ and $K_{IC}$

As described in section 2.1, the purpose of these tests was to examine the relation between $K_I$ and $K_{IC}$. In the following figure $K_{IC}$ is shown as a function of $K_I$. In all the figures a 45 degree line is inserted. The value of $K_{IC}$ should be above this line, unless the value of $K_I$ has reached the critical value. In all tests it has been ensured that $K_I < K_{IC}$.

In the earlier work [94.1] it was shown that $K_{IC}$ was increasing with increasing $K_I$. In figure 2.4 all the test results are shown including the results of the earlier work, the results from the large specimens (B=30 mm) and the results from the small specimens (B=20 mm). We observe that the results from [94.1] are reproduced although there is a large scatter. We furthermore observe pronounced increase in $K_{IC}$ for increasing $K_I$, as expected. The test specimens with the small thickness (B=20mm) gave similar results. We may therefore conclude that we have plane strain conditions where $K_{IC}$ is independent of the thickness.

Fracture toughness
Hardox 400
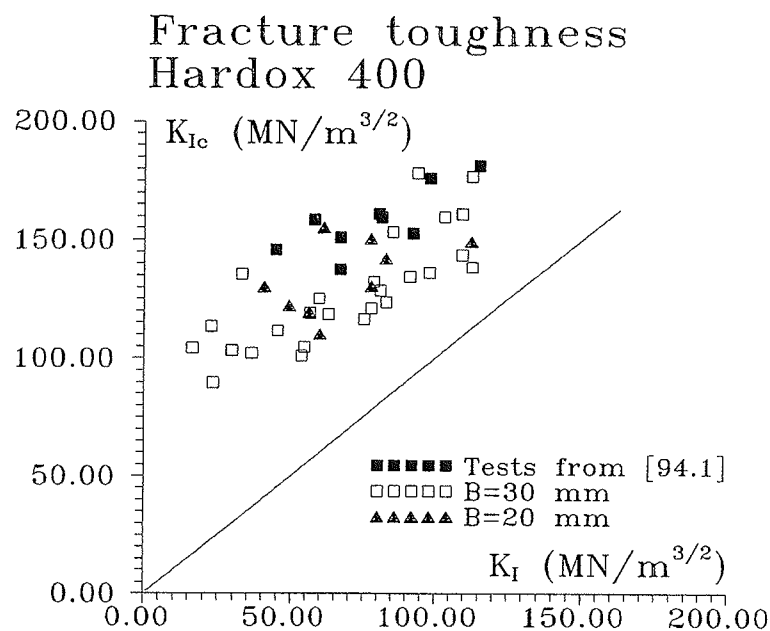


Figure 2.4

The fact that $K_{IC}$ increases for increasing $K_I$ has been observed in earlier tests, see for instance [70.1 p.52]. It is likely to assume, that the structure of the material in the plastic zone developed in front of the crack tip under cyclic loading is depending upon the value $K_I$ under crack initiation. One may for instance imagine that in the plastic zone, which is subjected to very large stresses, hardening of the material takes place. The hardening thus is a function of $K_I$.

Changes in the structure of the material due to the hardening will influence the critical stress intensity factor $K_{IC}$. It is therefore natural to assume that the critical stress intensity factor, which indeed depends on the fracture zone structure, must depend on $K_I$.

A variation of the crack length does not affect the results as can be seen from figure 2.5, where $K_{IC}$ is shown as function of the crack length. It may therefore be concluded that the critical stress intensity factor $K_{IC}$ depends on the actual stress intensity factor $K_I$ during fatigue loading.

The results will be treated in more detail in chapter 4.



Figure 2.5 *$K_{IC}$ as a function of the crack length*

7

# Chapter 3

## Fatigue tests

## 3.1　Introduction

In this chapter the fatigue tests will be described and the test results presented. The purpose of the tests is to measure the crack propagation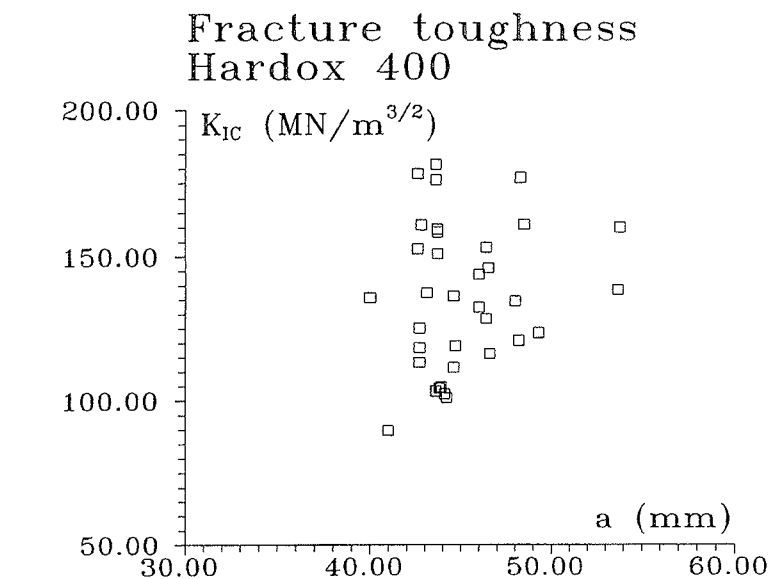 in the test specimens loaded by a dynamic load, and to determine the relation between the change in crack length per cycle **da/dN** and the stress intensity factor $K_I$. The crack length is measured with a Digital Image Processing System.

The fatigue tests were performed on the Swedish high strength steel Hardox 400 (see appendix B). In the earlier work **[94.1]** it was found that the crack propagation velocity da/dN was very high. The Paris m - value was measured to about m = 7, (steel normally obtains m=3). In the earlier work the specimens tested were very thin (B=2 mm). The manufacturing of these very thin plates might have effected the material in a way which caused the very high crack propagation rate. To examine this two different specimens were tested. The dimensions of both specimens were the same as the specimens used in the earlier project **[94.1]**. One specimen type was manufactured under exactly the same conditions as before in order to reproduce the original results. The other specimen type was cold treated during the manufacturing. All specimens were prepared from a 4 mm thick Hardox 400 plate. First the specimens were grinned down to the thickness 2 mm. Hereafter the specimens were polished on each side to ensure very low roughness. A number of 5 specimens were produced of each type. The test specimens used in the fatigue tests are shown in figure 3.1. They are of the type called the Center Crack Test specimen (CCT).
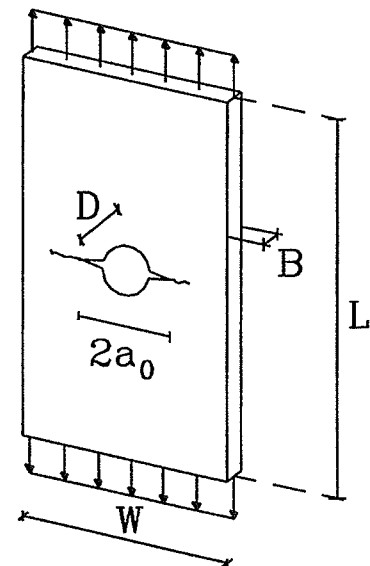


Figure 3.1 *Center Crack Test specimen (CCT)*

8

The dimensions of the tests specimens are shown in table 3.1.

| [mm] | $a_0$ | D | B | W | L |
|---|---|---|---|---|---|
| Hardox 400 | 8 | 8 | 2 | 80 | 180 |

Table 3.1 *Dimensions of the CCT specimens*

The specimens are numbered with two digits, xx, the first one indicates the thickness, 2 for B=2 mm, the second one indicates the test specimen number. For instance 23 is test specimen 3 with a thickness of B=2 mm. Furthermore the specimens which are cold treated during manufacturing are marked with a capital C, for instance C27.

## 3.2 Test results

In this section the test results from the fatigue tests will be presented. Test equipment and test procedure is described in detail in [94.1].
The values of the load increment $\Delta P$ and the frequency f used in the fatigue tests are shown in table 3.2.

| Hardox 400 | $P_{min}$ [N] | $P_{max}$ [N] | $\Delta P = P_{max} - P_{min}$ [N] | f [Hz] |
|---|---|---|---|---|
| B=2 mm | 2500 | 37500 | 35000 | 22.8 |

Table 3.2 *Load and frequency in the fatigue tests*

In the fatigue tests the crack length **a** and the number of cycles **N** are measured. Using these results the crack velocity **da/dN** may be determined by the relation:

$$\frac{da}{dN} = \frac{a_{i+1} - a_i}{N_{i+1} - N_i} \qquad (3.1)$$

The value of $a_i$ is chosen by the condition that for each calculated da/dN-value $a_{i+1} - a_i > 1$mm. This is done to ensure that at least 3 to 4 measured points are influencing the calculation of da/dN in order to minimize the uncertainty. The critical

9

crack length is about 25 mm, and about 30 crack lengths have been measured in each test.

The test data are given in appendix D, and they are presented graphically in this section. The crack growth is shown in figure 3.2. A total of 4 specimens (not cold treated) and 4 test specimens (cold treated) were tested succesfully.
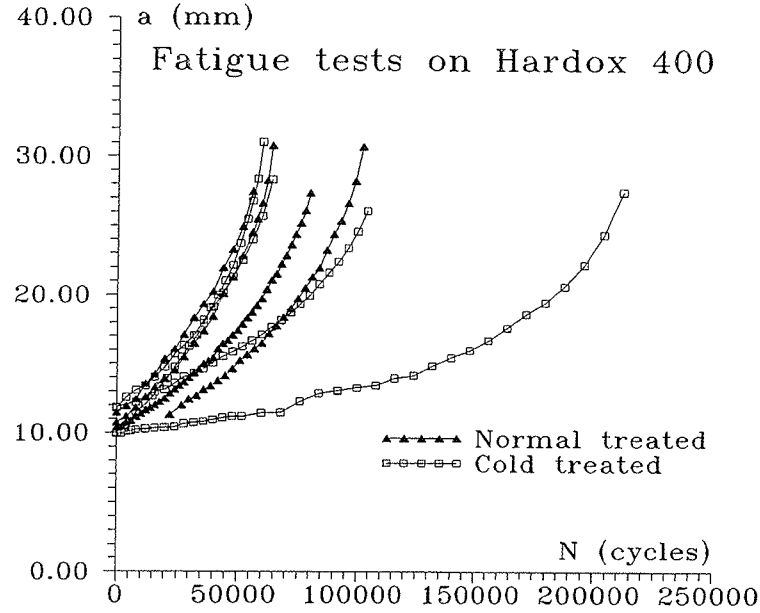


Figure 3.2 *Crack propagation versus number of cycles*

To calculate the crack velocity **da/dN** as a function of the stress intensity factor $K_I$, $K_I$ is determined by the equation, **[86.1]**:

$$K_I = \beta \sigma \sqrt{\pi a} \sqrt{\sec(\frac{\pi a}{W})} \qquad (3.2)$$

Here $\beta$ is a geometrical correction parameter due to the hole at the crack in the specimen, see figure 3.1. The parameter $\beta$ is given by the equation, **[75.1]**:

10

$$\beta = \left( 0.94 + \frac{0.34}{0.14 + \dfrac{a - D/2}{D}} \right) \qquad (3.3)$$

The calculated da/dN-curves for all the tests are presented in figure 3.3. It was observed during the tests that among the cold treated test specimens two of the specimens (C22 and C27) had a very long initiation time $N_i \approx 120000$ cycles before initiation of the crack. The two other cold treated specimens had an initiation time in the same range as the normal treated test specimen with 20000 cycles $< N_i < 45000$ cycles.
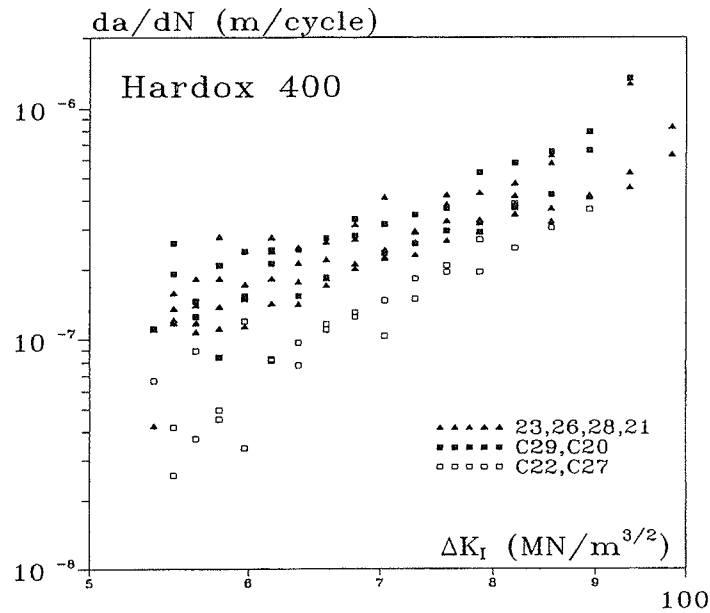


Figure 3.3 *Crack Propagation rate, da/dN-curve*

It is the same specimens (C22 and C27) which appear with a steeper slope and a low crack propagation rate in the da/dN-curve, figure 3.3. The purpose of the cold treated specimen was to reproduce the results from the earlier work [94.1]. It was not possible to reproduce these results. It must be concluded that the resistance of steel to fatigue is affected by the manufacturing procedure. However it seems that only two specimens were effected by the cold treatment. In the following the other two and the normal specimens will be considered as reliable results due to the fact

11

that they obtain a Paris **m** value equal to about **m** ≈ **3.09** as shown in figure 3.4, which is close to m = 3 as normally expected for steel.

The Paris equation **da/dN=C$\Delta$K$_I^m$**, where in this case $\Delta K_I \approx K_{Imax}$, is used to give an estimate of the relation between da/dN and $K_I$. The parameters C and m are calculated as an average for each test and the results are shown in the figure 3.4. These values will be used in the following chapter to make a first estimate of the parameters in the crack propagation formula.
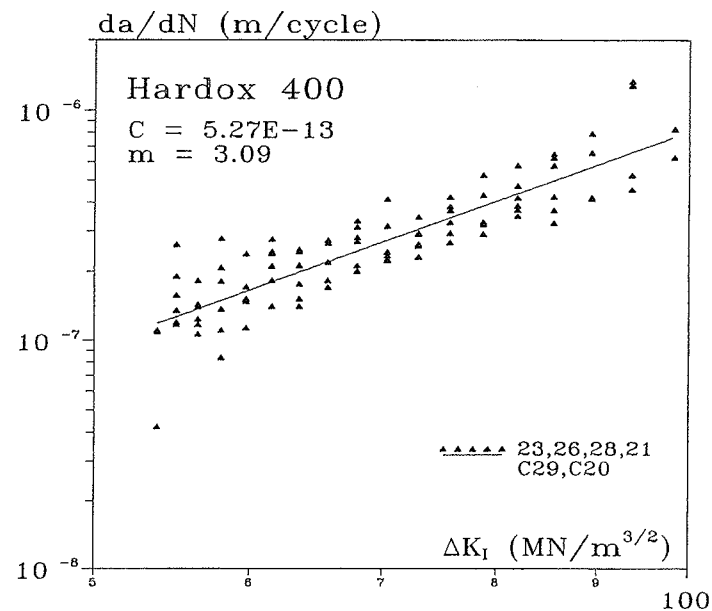


Figure 3.4 *Crack Propagation rate, da/dN-curve*

12

# Chapter 4

## Discussion of test results

In this chapter the test results presented in the previous chapters will be compared with the new theory, the Crack Propagation Formula (ECP), see formula (4.1).

$$\frac{da}{dP} = \frac{K_{I(a+l_e)}^2 \frac{\partial}{\partial P}\left(\frac{K_I^2}{2\pi f_y f_t}\right)}{K_{IC}^2 - K_{I(a+l_e)}^2} \tag{4.1}$$

The purpose is to follow-up upon the results presented in the earlier work [94.1]. Some parameters used in the formula will be taken from that work, other parameters will be determined in the following.

Firstly the relation between $K_I$ and $K_{IC}$ will be determined and used to determine $K_{IC}$ in the formula (4.1). Secondly the ultimate stresses will be determined, mainly on the basis of the Weibull size effect law (weakest link theory) and some considerations on the atomic strength of materials.

It is assumed that the $K_I$-$K_{IC}$-relation in general can be described by the equation (4.2), see [90.1]:

$$K_{IC} = M' K_I^{n'} \tag{4.2}$$

In the earlier work [94.1] the relation between $K_I$ and $K_{IC}$ was determined on the basis of very few tests results. In this paper several tests have been performed to verify the relation and to determine it more accurately. It was asumed in the earlier work that in the low range of $K_I$, $K_{IC}$ was decreasing with increasing $K_I$. The present work shows that $K_{IC}$ is increasing in the whole range of $K_I$, see chapter 2. This is also in agreement with the test results from the fatigue tests presented in chapter 3, where a best fit using the least square method gave the Paris m-value equal to m=3.09, see figure 3.4. This relates to a n'-value of about n'$\approx$ 0.5, see formula (4.3), which leads to increasing $K_{IC}$ for increasing $K_I$ according to formula (4.2).

$$m = 4 - 2 \cdot n' \text{ or}$$
$$n' = 2 - m/2 \tag{4.3}$$

There is a large scatter in the results of the $K_{IC}$ tests, see figure 4.1. It is quite complicated to make an optimization using the least square method, due to the fact that both $K_I$ and $K_{IC}$ are measured with a rather large uncertainty. A value of n' in the range 0.5 <n'< 0.3 gives a resonably good fit within the scatter band of the tests results. For n' = 0.4 and M'=25, which is approximately the same value as that used in the earlier work [94.1] in the range where $K_I$ is increasing. We observe that we get a good estimate of the $K_I$ - $K_{IC}$ relation, see figure 4.1. These values will be used in the following calculations.
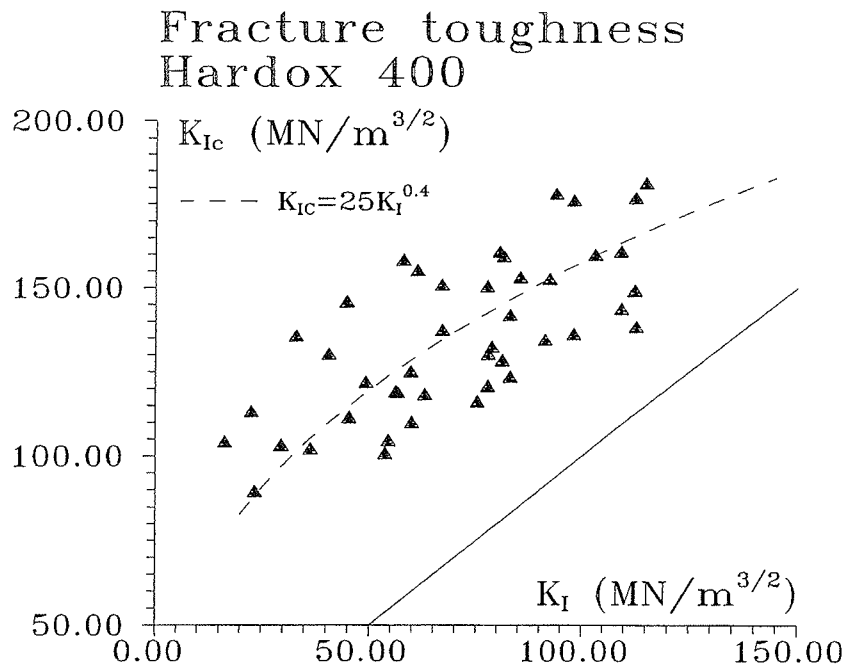


Figure 4.1 *Relation Between $K_I$ and $K_{IC}$*

As mentioned, it was not possible to measure a decrease in $K_{IC}$ for increasing $K_I$ for small values of $K_I$, as proposed by Davidson and Lankford [83.1], ( see also [94.1]). The reason might be that the crack propagation rate measured in the tests series in [94.1] was effected by the speciel treatment of the material used in manufacturing the specimens, which might have led to a mixed mode I and II fracture

in the tests specimens. It may be concluded that $K_{IC}$ is an increasing function of the stress intensity factor $K_I$ in the whole $K_I$-range.

In the following the ultimate strength of the material will be determined. The ultimate strength is highly dependent on size effects due to the very small plastic zone in front of the crack tip which leads to a higher strength in the plastic zone than that measured in laboratory tests. The phenomenon is described in detail in the earlier work by the author [94.1], and will only be summarized here.

The size effect is modelled using Weibull's size effect law, [39.1] and [39.2], together with some information on the atomic strength of the material. Weibull's size effect law can be written:

$$f_u = c \, V^{-\frac{1}{n}} \tag{4.4}$$

where the empirical parameters n and c can be determined on the basis of the atomic strength and laboratory strength by the following formulas, see [94.1]:

$$n = \frac{19.8}{\log\left(\dfrac{f_u^{\text{atomic}}}{f_u^{\text{laboratory}}}\right)} \tag{4.5}$$

$$c = f_u^{\text{laboratory}} L_0^{\frac{3}{n}}$$

Here $f_u$ is the ultimate strength, i.e. the yield strength $f_y$ and the fracture strength $f_t$ respectively and $L_0$ is the size of a laboratory test specimen which in [94.1] was set to $8 \cdot 10^{-3}$ m when determining the yield strength and $L_0 = 5 \cdot 10^{-3}$m due to the necked area, when determining the fracture strength $f_t$.
The atomic strength for steel related to the fracture strength is, see [94.1]:

$$f_t^{\text{atomic}} = 32000 \text{MPa} \tag{4.6}$$

15

The atomic yield strength may be put equal to:

$$f_y^{atomic} = 8300 MPa \qquad (4.7)$$

The laboratory strength for the material Hardox 400 was in [94.1] found to be:

$$f_y^{laboratory} = 1230 MPa$$
$$f_t^{laboratory} = 1730 MPa$$

The laboratory fracture strength $f_t^{laboratory}$ has to be increased with about 20% due to the fact that in a test we often get a combination of sliding failure along the edge and a separation failure in the necked area. The cleavage strength therefore will be higher than the average stress measured over the necked area leading to, see [94.1]:

$$f_t = 1.2 f_{truefracturestrength} \qquad (4.9)$$

When dealing with the yield strength, it is important to bear in mind that in plane strain the yield strength exceeds considerably the uniaxial yield strength. If the linear elastic stress distribution around a sharp crack is taken as the basis, the yield strength in plane strain is found to be 3 times the uniaxial yield strength [86.1,p 115]. Irwin suggested to use a factor of 1.68,[60.2]. In [90.1] the factor used was 2.4, a value which has been found on the basis of finite element calculations. Since this is probably the best estimate, we will use it here, i.e.,

$$f_{yoplanestrain} = 2.4 f_{youniaxial} \qquad (4.10)$$

This factor does not affect the determination of the Weibull parameter n, because n is determined on the basis of the actual uniaxial strength, but it does affect the determination of c which describes the actual stress condition in the case given. When the yield strength at the crack tip is found to be higher than the tensile strength at the crack tip, the yield strength must of course be put equal to the tensile strength.

According to formula (4.5) we get the following Weibull parameters for the fracture strength:

$$n = \frac{19.8}{\log\left(\dfrac{32000}{1.2 \cdot 1730}\right)} = \underline{16.7}$$

(4.11)

$$c = 1.2 \cdot 1730 \cdot (5 \cdot 10^{-3})^{\frac{3}{16.7}} = \underline{801}$$

and for the yield strength:

$$n = \frac{19.8}{\log\left(\dfrac{8300}{1230}\right)} = \underline{23.9}$$

(4.12)

$$c = 2.4 \cdot 1230 \cdot (5 \cdot 10^{-3})^{\frac{3}{23.9}} = \underline{1610}$$

In stead of using the Weibull roots **n** for the volume scale it has been suggested in [90.1] to use the length scale roots **n/3**. When this is done the length of the fracture zone might be used to determine the fracture strength $f_t$ at the crack tip and the length of the plastic zone may be used to calculate the yield stress at the crack tip, see [94.1].

From [94.1] we have the following equations for the ultimate strengths.
The formula for the yield strength is:

$$f_y = \left[ c \left( \frac{K_I^2}{2\pi} \right)^{-\frac{3}{n}} \right]^{\frac{1}{1 - \frac{6}{n}}}$$

(4.13)

17

For the fracture strength we have:

$$f_t = \left[ c \left( \frac{K_I^2}{2\pi f_y} \right)^{-\frac{3}{n}} \right]^{\frac{1}{1-\frac{3}{n}}}$$  (4.14)

With this approach it might be found that the theoretical yield strength $f_y$ exceeds the fracture strength $f_t$. In this case we may use $f_y = f_t$ in the crack tip.

The ultimate strengths depend on $K_I$, because the size of the plastic and fracture zone length depends on $K_I$, see equation (4.13) and (4.14). $K_I$ may be chosen as an average value in the interval in case. In our case $K_I$ varies from about 45 $MN/m^{3/2}$ to 95 $MN/m^{3/2}$. As an average we may put $K_I = 70$ $MN/m^{3/2}$ in the calculations.

Using formulas (4.13) and (4.14) we get the ultimate strengths:

$$\begin{aligned} f_y &= 6267\,MPa \\ f_t &= 5466\,MPa \end{aligned}$$  (4.15)

Since $f_t$ is found less than $f_y$ we must use:

$$f_y = f_t = 5466\,MPa$$  (4.16)

In the following the parameters shown in table 4.1 will be used to predict the crack propagation behaviour of the CCT specimens:

| D | $a_0$ | M' | n' | $f_t$ |
|---|---|---|---|---|
| 8 mm | 8 mm | 25 | 0.4 | 5466 MPa |

Table 4.1 *Parameters for Center Cracked Test specimen.*

In the table $a_0$ is half the initial crack length and D the diameter of the hole at the crack center, see figure 3.1.

In figure 4.2 the test results are compared with the Energy Crack Propagation Formula (ECP). It is observed that the theory predicts much higher crack growth rate than found in the tests.
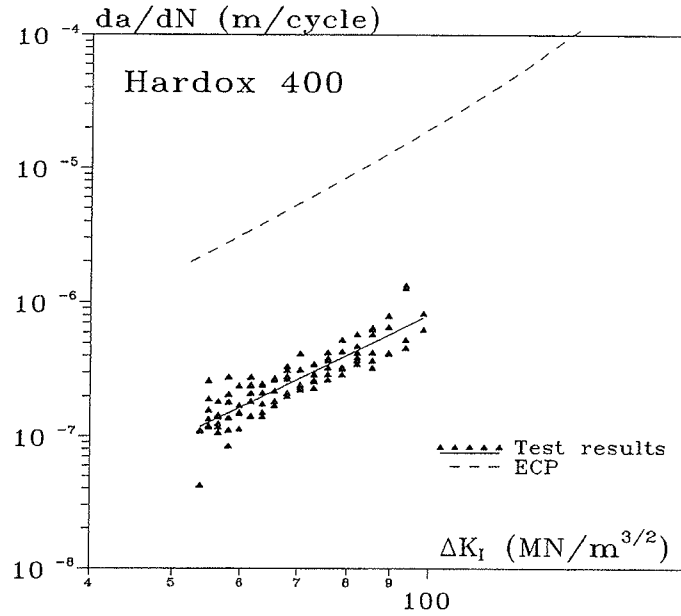


Figure 4.2 *Theory compared with test results.*

To examine the possible reasons for this discrepancy we begin by studying the effect of small changes in the parameters used. Firstly the relation between $K_{IC}$ and $K_I$ is studied. We may, within the range of the test data, choose extreme values of n' and M'as those given in table 4.2, where M' has been determined using the average value $\Delta K_I \approx 70$ MN/m$^{3/2}$, i.e.

$$M' = 25 \cdot 70^{0.4-n'}$$   (4.17)

| n' | M' | $f_t \approx f_y$ |
|---|---|---|
| 0.4 | 25 | 5466 |
| 0.2 | 58 | 5466 |
| 0.6 | 11 | 5466 |

Table 4.2 *Parameters used to determine the $K_{IC}$-$K_I$ relation.*

19

These values leads to the extreme $K_{IC}$-$K_I$ relations shown in figure 4.3.
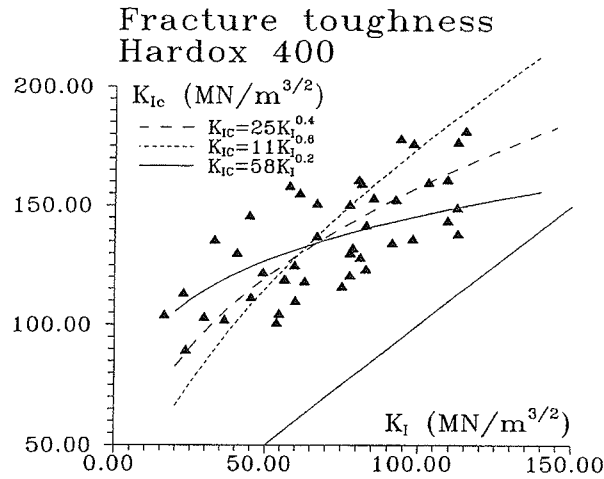


Figure 4.3 *Relation between $K_{IC}$ and $K_I$ for different value of n'.*

In figure 4.4 the extreme values of n' and M' have been used to determine the crack propagation behaviour.
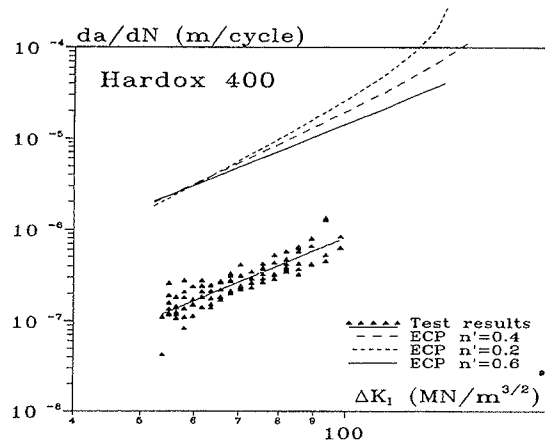


Figure 4.4 *Theory compared with test results.*

We observe that this does not influence the results very much.

If n' and M' are estimated on the basis of the Paris m-value and the $K_{IC}$-values from the fatigue test, using the values:

$$m \approx 3.06 \quad \text{and} \quad 120 \text{ MN/m}^{3/2} < K_{IC} < 150 \text{ MN/m}^{3/2}$$

we get:

20

$$n' = 2 - 0.5\,m = 0.45$$

$$M' = \frac{120}{120^{0.6}} = 7$$

$$M' = \frac{150}{150^{0.2}} = 55$$

(4.18)

Since M' must be lying somewhere in between 55 and 7, we may conclude that our choice M' = 25 and n' = 0.4 may be considered reasonable, and that a change within a reasonable range does not affect the results very much.

The influence from the ultimate strengths will now be examined. In figure 4.5 calculations with ECP using the ultimate strengths $f_u = f_t \approx f_y \approx 10000$ MPa and 20000 MPa respectively are shown.
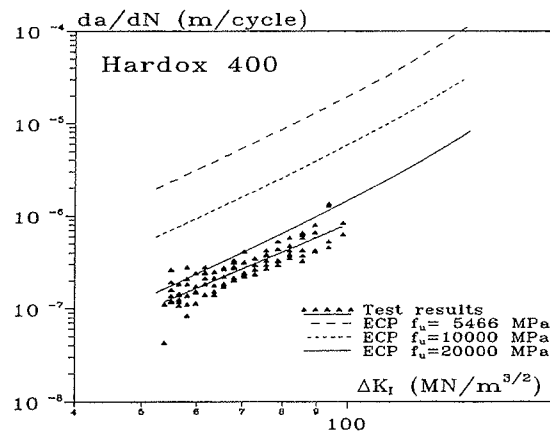


Figure 4.5 *Theory compared with test results.*

It is observed that putting the ultimate strengths equal to 20000 MPa the theory does predict the crack propagation behaviour well. An increase of the ultimate strengths might be quite natural, because the hardening taking place in the fracture zone and in the plastic zone will of course affect not only the $K_{IC}$-value but also the strength values. This effect has not yet been taken into account. However a strength of 20000 MPa approaches the atomic strength and it does not seem likely that hardening may have such a pronounced effect.

We must conclude that better agreement can not in a reasonable way be obtained by changing the parameters of the model.

If we compare the fatigue test results obtained here with typical da/dN - $\Delta K_I$ curves for other types of steel [91.1], see figure 4.6, we observe that steel with a medium strength (A470 and AISI) gives similar results as the Hardox steel and we observe that high strength steel (Commercial) gives higher crack propagation rates, although high ultimate strength should lead to lower crack propagation rate according to ECP unless the $K_{IC}$-value is decreased correspondingly. Normally this is the case. It is well-known that most steels have crack growth rates which lead to a rather narrow scatter band. However this pattern seems to be violated by ductile steels with low strength and by the Hardox steel treated here. For the low strength, ductile steels there will be substantial plastic deformations at the crack tip.
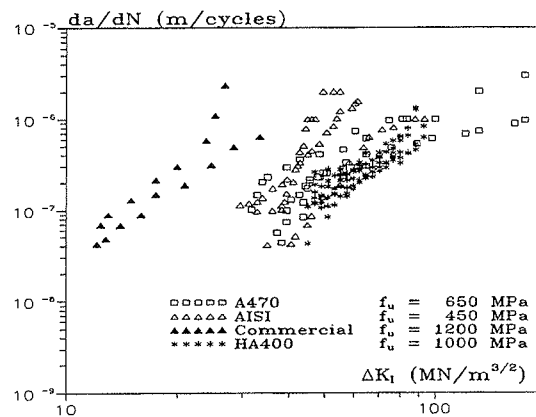


Figure 4.6 *Comparison of different steel alloys.*

The low crack growth rates for ductile low strength steels and maybe our Hardox steel may be explained by a phenomenon called crack closure. Crack closure has been treated by the author in [96.1] and for detailed information the reader is referred to [95.1]. In the following the effects of crack closure will be shortly summarized.

Because of the plastic deformations the crack will close during unloading before the specimen is totally unloaded. Since the crack is open only for a part of the loading sequence an effective stress intensity factor range $\Delta K_{eff} = K_{Imax} - K_{op}$ is governing the crack growth, $K_{op}$ being the stress intensity factor when the crack starts to open and the crack starts to propagate. This explains the delay of crack propagation caused by overloading. Furthermore the crack propagation is delayed in general and is to some degree a function of $\Delta K_{eff}$ instead of $\Delta K_I$. If the R ratio,

22

i.e. the $P_{min}/P_{max}$ ratio is high the effect will be reduced, because $K_{Imin}$ approaches $K_{op}$ and the effective stress range $\Delta K_{eff}$ equals $\Delta K_I$.

Elber [71.2] was the first to describe this phenomenon. He suggested the simple relation:

$$\Delta K_{eff} = (0.5 + 0.4R) \Delta K_I \qquad (2.37)$$

where $\Delta K_{eff}$ should be used in stead of $\Delta K_I$ in the crack propagation formulas, like the Paris formula, i.e.

$$\frac{da}{dN} = C\Delta K_{eff}^m \qquad (2.38)$$

In the tests described in this paper $\sigma_{min}$ is very small and we may consider $R \approx 0$. As a rough estimate we may use a method suggested in [96.1] valid for normal strength steel. The method take the effect of crack closure into account by using a reduced, effective stress intensity factor $K_{eff} = K_{Imax} - K_{op}$ in the calculation, where $K_{op}$ is determined by the crack opening stress at the crack tip, $S_o$, which approximately can be put equal to $S_o \approx 0.3 \cdot \sigma_{max}$. In Elbers expression we have $S_o = 0.5 \cdot \sigma_{max}$ for $R = 0$. Since we do not know the exact effect of crack closure in the Hardox 400 tests, both the factor 0.3 and 0.5 has been used in the calculations shown in figure 4.7.
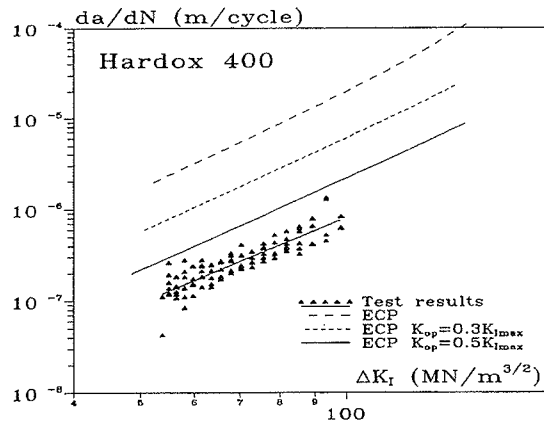


Figure 4.7 *Effect of crack closure compared with test results.*

23

We observe that crack closure may explain why the predicted crack propagation rate is too high. However much more research is needed before any final conclusion may be taken.

# Chapter 5

# Recommendations for future research

There are many subjects which should be researched more in connection with the further evaluation of the Energy Balance Crack growth formula.
The most important ones are:

1) The fracture strength and the yield strength at the crack tip.
It is possible that the cleavage strength is highly underestimated and that the yield strength is overestimated by using the Weibull size effect theory. As mentioned in [94.1] it has been found in some cases that the atomic cleavage strength is reached already at a length scale of 1 µm. On the other hand the Weibull theory may be extended too far, when used for scaling the yield strength. The effect of hardening on the strength parameters, tensile strength and yield strength, should also be studied.

2) The influence of the microstructure of the steel.
It is likely that account must be taken of parameters like grain size, strength in the grains and along grain boundaries, influence of foreign atoms on the atomic strength, number and type of dislocations etc. These parameters of course influence the parameters already used is the equation, but it should be investigated whether other parameters could be included. For instance the order of magnitude of the crack extension in one cycle is $10^3$ atomic distances. Thus a number of foreign atoms will be activated in one crack extension step, which could mean that the strength to be used is the crack growth formula should include the effect of foreign atoms. It is also to be expected that things will be different whether one crack extension step is within the grain size or include more grains.

24

3) <u>The mechanism of crack growth.</u>
   Much work has been done in this area. In relation to the crack growth formula two extreme mechanisms should be examined further. The one, which has been tacitly assumed, is that the whole process zone is moving in the direction of the crack axis. For some materials, for instance very ductile ones, other mechanisms should be studied, for instance a mechanism where the yield zone is unchanged in a number of crack extension steps and failure is by local crack development in the yield zone.

4) <u>The effective crack length.</u>
   It must be admitted that the determination of the effective crack length has been done by very rough methods. More refined methods should be introduced and used to evaluate the present way of calculating the effective crack length.

5) <u>The effect of crack closure.</u>
   In this paper it has been suggested that by including crack closure better agreement might be obtained for low and medium strength steels. If the basic ideas of the model can be maintained, the effect of crack closure should be taken into account along the lines mentioned searching for improved values of the crack opening stress intensity factor.

# Chapter 6

# Conclusion

This paper is a follow-up on the work [94.1]. The main purpose has been to further evaluate the basic concepts of the Energy Crack Propagation Formula (ECP), and to examine the capability of ECP to predict crack propagation behaviour.

As a main conclusion it has been verified that the critical stress intensity factor $K_{IC}$ varies with the stress intensity level. It has been shown that this dependency may be used to calculate the slope of the $da/dN$-$\Delta K_I$ curve, which means that it is possible to calculate the Paris m value.

The level of crack propagation rate is highly dependent on the ultimate strength and the critical stress intensity factor $K_{IC}$. It has been shown, that for the steel tested, ECP can not estimate the level of the crack propagation rate in its present form. Several parameters influence the fracture mechanical parameters, such as microstructure, size effects, hardening of the material etc. It is necessary to perform further research in these areas in order to understand the effect on the fracture mechanical parameters.

The effect of crack closure has been investigated. It was shown that to some extent this may explain the delay in fatigue crack growth, but much more research is needed in this field before any final conclusion may be drawn.

The Energy Crack Propagation formula (ECP) has been shown to be able to predict crack propagation in different metals in this and the earlier work, when the correct fracture mechanical parameters are used. Therefore the model can be recommended for future research to understand the mechanisms of fatigue and crack propagation. Even more research is needed before it can be used for practical applications.

# Appendix A

## Reference list

[39.1] W.Weibull, *A statistical theory of the strength of materials*, Ingeniörvetenskapsakadamien. Handlingar nr 151, 1939

[39.2] W.Weibull, *The phenomenon of rupture in materials*, Ingeniörvetenskapsakadamien. Handlingar nr 153, 1939

[70.1] W.F.Brown, *Review of developments in plane strain fracture toughness testing*, ASTM STP 463, 1970.

[71.2] W.Elber, *The significance of fatigue crack closure*, Damage Tolerance in Aircraft Structures, ASTM STP 486, p 230-42, 1971.

[83.1] D.L.Davidson and J.Lankford, *Fatigue Crack Tip Strains in 7075-T6 Aluminum Alloy by Stereoimaging and their Use in Crack Growth Models*, ASTM STP 881, pp 371-399, 1983.

[86.1] D.Broek, *Elementary engineering fracture mechanics*, FractuREsearch Inc. Galena, OH, USA, 1986.

[90.1] M.P.Nielsen, *An energy balance crack growth formula*, Bygningsstatiske meddelelser nr 3-4, Dansk Selskab for Bygningsstatik, Sept 1990.

[91.1] H.H.Pedersen and T.C.Hansen, *Revnevækst i stål*,(Crack Propagation in steel), M.Sc.Thesis, Department of Structural Engineering, Technical University of Denmark, Feb 1991.

A1

**[92.1]** J.Lyngbye, *Applications of digital image analysis in experimental mechanics*, PH.D.-thesis, Instituttet for Bygningsteknik, AUC, Aalborg, Denmark, May 1992.

**[94.1]** T.C.Hansen, *Fatigue and Crack Propagation, A new approach to predict crack propagation behavior*, Department of Structural Engineering, Technical University of Denmark, Report R316, June 1994.

**[95.1]** J.B.Ibsø, *Fatigue Life Prediction of Welded Joints Based on Fracture Mechanics and Crack Closure*, Series R No 322, Department of Structural Engineering, Technical University of Denmark, 1995.

**[96.1]** T.C.Hansen, *Fatigue in Welded Connections, A new approach to predict crack propagation behavior*, Department of Structural Engineering, Technical University of Denmark, Report R10, November 1996.

**[96.2]** T.C.Hansen and D.H.Olsen, *Fracture and crack growth in Concrete, A new approach to predict crack propagation behavior*, Department of Structural Engineering, Technical University of Denmark, Report R11, November 1996.

# Appendix B

## Material descriptions

## High strength steel Hardox 400

**Producer**     Swedish Steel Oxelösund
Box 1000
61301 Oxelösund
Sweden

**Usage**     Hard wearing steel. Used in trucks, buldozers, wheel constructions and much more.

**Composition**
(in %)

| C | Si | Mn | P | S | Cr | Mo | B |
|---|---|---|---|---|---|---|---|
| 0.20 | 0.10-0.70 | 1.70 | 0.025 | 0.01 | 0.80 | 0.80 | 0.005 |

The remainder is steel, the steel is fine grain treated.
The values are maximum values.

**Strength**
Factory
Values

| Yield strength | Ultimate strength | Elongation |
|---|---|---|
| 1000 MPa | 1250 MPa | 10 % |

# Appendix C

## Data from the $K_{IC}$ standard tests

In this appendix all the test results from the $K_{IC}$ standard tests are presented. The data include the crack length **a** initiated under a dynamic load $\Delta P = P_{max} - P_{min}$, the critical load $P_{cr}$, and finally the calculated $K_I$ and $\Delta K_I$ value under initiation and the critical $K_{IC}$ value at fracture. The following expression [86.1] has been used:

$$K_I = \frac{P}{B \cdot W^{1/2}} \left( 29.6 \left( \frac{a}{W} \right)^{1/2} - 185.5 \left( \frac{a}{W} \right)^{3/2} \right.$$
$$\left. + 655.7 \left( \frac{a}{W} \right)^{5/2} - 1017 \left( \frac{a}{W} \right)^{7/2} + 638.9 \left( \frac{a}{W} \right)^{9/2} \right)$$

Regarding notation, see section 2.1. $K_{IC}$ is calculated using $P_{cr}$ and a, while $\Delta K_I$ is calculated using $\Delta P$ and a.

| (mm) | B | W |
|------|---|---|
| small HA400 | 20 | 47.5 |
| large HA400 | 30 | 80 |

Some of the tests are not valid due to the reasons listed below.

1) Test 41 was loaded dynamically. At the end of the dynamic test the test machine could not keep the loading level which led to smaller load than expected. The results can't be considered as reliable and are not used in the report.

Units:
$[a]=mm; [P]=kN; [K_I]=MN/m^{3/2}$

| large Ha400 | $a_0$ | $P_{max}$ | $\Delta P$ | $P_{cr}$ | $K_I$ | $\Delta K_I$ | $K_{Ic}$ |
|---|---|---|---|---|---|---|---|
| 10 | 48.5 | 66.8 | 60 | 98.3 | 109.33 | 98.2 | 160.9 |
| 11 | 46.0 | 75.4 | 71.3 | 99.2 | 109.35 | 103.4 | 143.8 |
| 12 | 42.6 | 75.0 | 71.4 | 142.3 | 93.91 | 89.4 | 178.2 |
| 13 | 42.7 | 50.1 | 45.7 | 94.2 | 63.04 | 57.5 | 118.4 |
| 14 | 41.0 | 20.0 | 13.2 | 76.3 | 23.48 | 15.5 | 89.7 |
| 15 | 43.6 | 22.8 | 16.8 | 79.1 | 29.59 | 21.8 | 103.2 |
| 16 | 44.1 | 27.3 | 20.6 | 76.7 | 36.44 | 27.5 | 102.2 |
| 17 | 42.7 | 18.1 | 13.5 | 90.1 | 22.66 | 16.9 | 113.3 |
| 18 | 40.0 | 29.2 | 22.9 | 119.9 | 33.03 | 25.9 | 135.7 |
| 19 | 44.6 | 33.3 | 26.9 | 81.9 | 45.31 | 36.6 | 111.5 |

| large HA400 | $a_0$ | $P_{max}$ | $\Delta P$ | $P_{cr}$ | $K_I$ | $\Delta K_I$ | $K_{Ic}$ |
|---|---|---|---|---|---|---|---|
| 20 | 43.8 | 12.5 | 8.34 | 79.2 | 16.44 | 10.97 | 104.2 |
| 21 | 44.2 | 40.9 | 35.9 | 75.4 | 53.66 | 47.1 | 100.9 |
| 22 | 42.7 | 47.5 | 41.9 | 99.5 | 59.74 | 52.7 | 125.1 |
| 23 | 43.9 | 42 | 37.4 | 79.2 | 55.48 | 49.4 | 104.7 |
| 24 | 44.7 | 41.4 | 35.7 | 86.9 | 56.59 | 48.8 | 118.9 |
| 25 | 53.8 | 46.9 | 38.6 | 72.7 | 103.16 | 84.9 | 159.9 |
| 26 | 48.2 | 48.3 | 43.2 | 74.5 | 77.82 | 69.6 | 120.8 |
| 27 | 49.3 | 48.7 | 42.4 | 72.5 | 83.04 | 72.3 | 123.6 |
| 28 | 46.4 | 54.9 | 48.9 | 86.9 | 81.06 | 72.2 | 128.4 |
| 29 | 53.7 | 51.6 | 43.4 | 63.3 | 112.83 | 94.9 | 138.4 |

| large HA400 | $a_0$ | $P_{max}$ | $\Delta P$ | $P_{cr}$ | $K_I$ | $\Delta K_I$ | $K_{Ic}$ |
|---|---|---|---|---|---|---|---|
| 30 | 46.4 | 57.8 | 51.7 | 103.7 | 85.41 | 76.4 | 153.2 |
| 31 | 48 | 57.2 | 51.7 | 84.3 | 91.28 | 82.5 | 134.5 |
| 32 | 46 | 54.2 | 49 | 91.3 | 78.65 | 71.1 | 132.4 |
| 33 | 44.6 | 72 | 66 | 100 | 98.07 | 89.9 | 136.2 |
| 34 | 48.3 | 69.5 | 63.2 | 109.4 | 112.61 | 102.4 | 176.9 |
| 35 | 46.6 | 50.5 | 45.1 | 77.9 | 75.25 | 67.2 | 116.2 |

A6

| small HA400 | $a_0$ | $P_{max}$ | $\Delta P$ | $P_{cr}$ | $K_I$ | $\Delta K_I$ | $K_{Ic}$ |
|---|---|---|---|---|---|---|---|
| 40 | 32.9 | 16.4 | 14.4 | 31.8 | 77.67 | 68.2 | 150.5 |
| 41[1] | 36.7 | 17.1 | 15.3 | 16.3 | 125.62 | 112.4 | 119.4 |
| 42 | 30.8 | 20.4 | 16 | 34.1 | 77.90 | 61.1 | 130.3 |
| 43 | 32.5 | 24.8 | 19.4 | 32.9 | 112.49 | 88 | 149.3 |
| 44 | 30.4 | 11.1 | 8.2 | 35.4 | 40.61 | 30 | 130.2 |
| 45 | 33.9 | 9.4 | 5.1 | 23.1 | 49.21 | 26.7 | 121.9 |
| 46 | 34.2 | 15.2 | 10.9 | 26 | 82.97 | 59.5 | 142 |
| 47 | 32.5 | 13.5 | 10.3 | 34.2 | 61.21 | 46.7 | 155.2 |
| 48 | 32.5 | 12.4 | 7.9 | 26.3 | 56.19 | 35.8 | 119.3 |
| 49 | 37 | 7.9 | 3.44 | 14.5 | 59.94 | 26.1 | 110.1 |

*note 1: The test is not valid.*

# Appendix D

## Data from the fatigue tests

In this appendix all the test results from the fatigue tests are presented, i.e. the measured crack length **a** as function of number of cycles **N**.

All test specimens were loaded dynamically with $\Delta P = 37500 - 2500$ N = 35000 N, at the frequency f= 22.8 Hz.

A number of 10 test specimens were manufactured of Hardox steel, specimens 20-29. 5 test specimens were cold treated in the manufacturing fase.

Two tests were not valid due to the reasons listed below.

1)    The crack propagated asymmetrically in specimen 25 which led to unreliable results.

2)    Specimen 24 was subjected to compression by a mistake, and the specimen failed in buckling, and could therefore not be tested in fatigue.

Test results from these tests are not used in the report.

Units:
[a]=mm; [N]=Number of cycles;

| Specimen cct20; Cold treated | | | | |
|---|---|---|---|---|
| Crack initiation: $N_i$ = 36000; | | | | |
| | meas/a = 10.1 | | meas/a = 13.2 | |
| N | meas | a [mm] | meas | a [mm] |
| 0 | 126 | 12.47524 | 147 | 11.13636 |
| 4000 | 133 | 13.16831 | 158 | 11.96969 |
| 8000 | 140 | 13.86138 | 162 | 12.27272 |
| 12000 | 143 | 14.15841 | 167 | 12.65151 |
| 16000 | 150 | 14.85148 | 174 | 13.18181 |
| 20000 | 156 | 15.44554 | 185 | 14.01515 |
| 24000 | 165 | 16.33663 | 199 | 15.07575 |
| 28000 | 172 | 17.0297 | 206 | 15.60606 |
| 32000 | 180 | 17.82178 | 215 | 16.28787 |
| 36000 | 195 | 19.30693 | 225 | 17.04545 |
| 40000 | 204 | 20.19801 | 238 | 18.0303 |
| 44000 | 215 | 21.28712 | 251 | 19.01515 |
| 48000 | 228 | 22.57425 | 265 | 20.07575 |
| 52000 | 240 | 23.76237 | 280 | 21.21212 |
| 56000 | 257 | 25.44554 | 297 | 22.50 |
| 60000 | 276 | 27.32673 | 317 | 24.01515 |
| 64000 | 310 | 30.69306 | 342 | 25.90909 |

A9

| Specimen cct21; Normal treated | | | | |
|---|---|---|---|---|
| Crack initiation: $N_i$ = 32000; | | | | |
| | meas/a = 10.3 | | meas/a = 13.2 | |
| N | meas | a [mm] | meas | a [mm] |
| 0 | 121 | 11.74757 | 148 | 11.21212 |
| 4000 | 126 | 12.233 | 154 | 11.66666 |
| 8000 | 131 | 12.71844 | 160 | 12.12121 |
| 12000 | 143 | 13.88349 | 174 | 13.18181 |
| 16000 | 147 | 14.27184 | 187 | 14.16666 |
| 20000 | 162 | 15.72815 | 197 | 14.92424 |
| 24000 | 168 | 16.31067 | 208 | 15.75757 |
| 28000 | 182 | 17.6699 | 218 | 16.51515 |
| 32000 | 193 | 18.73786 | 237 | 17.95454 |
| 36000 | 206 | 20 | 246 | 18.63636 |
| 40000 | 215 | 20.87378 | 259 | 19.62121 |
| 44000 | 235 | 22.81553 | 278 | 21.0606 |
| 48000 | 248 | 24.07766 | 296 | 22.42424 |
| 52000 | 267 | 25.92233 | 316 | 23.93939 |
| 56000 | 300 | 29.12621 | 340 | 25.75757 |

| Specimen cct22; Cold treated | | | | |
|---|---|---|---|---|
| Crack initiation: $N_i$ = 118000; | | | | |
| | meas/a = 10.6 | | meas/a = 13.1 | |
| N | meas | a [mm] | meas | a [mm] |
| 0 | 108 | 10.18867 | 127 | 9.694656 |
| 2000 | 108 | 10.18867 | 127 | 9.694656 |
| 4000 | 110 | 10.37735 | 128 | 9.770992 |
| 6000 | 110 | 10.37735 | 130 | 9.923664 |
| 8000 | 111 | 10.47169 | 131 | 10 |
| 12000 | 112 | 10.56603 | 131 | 10 |

A10

| Specimen cct22; Cold treated | | | | |
|---|---|---|---|---|
| Crack initiation: $N_i$ = 118000; | | | | |
| | meas/a = 10.6 | | meas/a = 13.1 | |
| N | meas | a [mm] | meas | a [mm] |
| 16000 | 113 | 10.66037 | 131 | 10 |
| 20000 | 113 | 10.66037 | 132 | 10.07633 |
| 24000 | 113 | 10.66037 | 134 | 10.229 |
| 28000 | 116 | 10.94339 | 136 | 10.38167 |
| 32000 | 117 | 11.03773 | 137 | 10.45801 |
| 36000 | 118 | 11.13207 | 138 | 10.53435 |
| 40000 | 120 | 11.32075 | 139 | 10.61068 |
| 44000 | 122 | 11.50943 | 140 | 10.68702 |
| 48000 | 122 | 11.50943 | 143 | 10.91603 |
| 52000 | 122 | 11.50943 | 143 | 10.91603 |
| 60000 | 127 | 11.98113 | 143 | 10.91603 |
| 68000 | 128 | 12.07547 | 143 | 10.91603 |
| 76000 | 135 | 12.73584 | 155 | 11.83206 |
| 84000 | 144 | 13.5849 | 159 | 12.1374 |
| 92000 | 147 | 13.86792 | 161 | 12.29007 |
| 100000 | 148 | 13.96226 | 165 | 12.59541 |
| 108000 | 149 | 14.0566 | 168 | 12.82442 |
| 116000 | 156 | 14.71698 | 173 | 13.2061 |
| 124000 | 157 | 14.81132 | 177 | 13.51145 |
| 132000 | 167 | 15.75471 | 183 | 13.96946 |
| 140000 | 174 | 16.41509 | 190 | 14.50381 |
| 148000 | 180 | 16.98113 | 196 | 14.96183 |
| 156000 | 189 | 17.83018 | 204 | 15.57251 |
| 164000 | 203 | 19.15094 | 211 | 16.10687 |
| 172000 | 216 | 20.37735 | 221 | 16.87022 |
| 180000 | 227 | 21.41509 | 229 | 17.48091 |
| 188000 | 241 | 22.73584 | 243 | 18.54961 |

A11

| Specimen cct22; Cold treated | | | | |
|---|---|---|---|---|
| Crack initiation: $N_i$ = 118000; | | | | |
| | meas/a = 10.6 | | meas/a = 13.1 | |
| N | meas | a [mm] | meas | a [mm] |
| 196000 | 261 | 24.62264 | 259 | 19.77099 |
| 204000 | 289 | 27.26415 | 281 | 21.45038 |
| 212000 | 332 | 31.32075 | 309 | 23.58778 |

| Specimen cct23; Normal treated | | | | |
|---|---|---|---|---|
| Crack initiation: $N_i$ = 42000; | | | | |
| | meas/a = 11.2 | | meas/a = 12.4 | |
| N | meas | a [mm] | meas | a [mm] |
| 0 | 120 | 10.71428 | 124 | 10 |
| 2000 | 121 | 10.80357 | 125 | 10.08065 |
| 4000 | 125 | 11.16071 | 128 | 10.32258 |
| 6000 | 127 | 11.33928 | 129 | 10.40322 |
| 8000 | 130 | 11.60714 | 133 | 10.7258 |
| 10000 | 133 | 11.875 | 135 | 10.88709 |
| 12000 | 136 | 12.14285 | 138 | 11.12903 |
| 14000 | 139 | 12.41071 | 139 | 11.20967 |
| 16000 | 142 | 12.67857 | 141 | 11.37096 |
| 18000 | 144 | 12.85714 | 144 | 11.6129 |
| 20000 | 148 | 13.21428 | 145 | 11.69354 |
| 22000 | 151 | 13.48214 | 151 | 12.17741 |
| 24000 | 155 | 13.83928 | 154 | 12.41935 |
| 26000 | 158 | 14.10714 | 158 | 12.74193 |
| 28000 | 160 | 14.28571 | 162 | 13.06451 |
| 30000 | 166 | 14.82142 | 163 | 13.14516 |
| 32000 | 170 | 15.17857 | 167 | 13.46774 |
| 34000 | 173 | 15.44642 | 170 | 13.70967 |
| 36000 | 179 | 15.98214 | 173 | 13.95161 |

A12

| Specimen cct23; Normal treated | | | | |
|---|---|---|---|---|
| Crack initiation: $N_i$ = 42000; | | | | |
| | meas/a = 11.2 | | meas/a = 12.4 | |
| N | meas | a [mm] | meas | a [mm] |
| 38000 | 181 | 16.16071 | 176 | 14.19354 |
| 40000 | 182 | 16.25 | 181 | 14.59677 |
| 42000 | 192 | 17.14285 | 185 | 14.91935 |
| 44000 | 199 | 17.76785 | 187 | 15.08064 |
| 46000 | 200 | 17.85714 | 192 | 15.48387 |
| 48000 | 206 | 18.39285 | 195 | 15.7258 |
| 50000 | 210 | 18.75 | 199 | 16.04838 |
| 52000 | 215 | 19.19642 | 205 | 16.53225 |
| 54000 | 220 | 19.64285 | 211 | 17.01612 |
| 56000 | 226 | 20.17857 | 214 | 17.25806 |
| 58000 | 233 | 20.80357 | 219 | 17.66129 |
| 60000 | 239 | 21.33928 | 224 | 18.06451 |
| 62000 | 243 | 22.0909 | 230 | 18.69918 |
| 64000 | 252 | 22.90909 | 236 | 19.18699 |
| 66000 | 256 | 23.27272 | 243 | 19.75609 |
| 68000 | 266 | 24.18181 | 249 | 20.2439 |
| 70000 | 274 | 24.90909 | 255 | 20.7317 |
| 72000 | 285 | 25.90909 | 262 | 21.30081 |
| 74000 | 295 | 26.81818 | 269 | 21.86991 |
| 76000 | 307 | 27.90909 | 276 | 22.43902 |
| 78000 | 319 | 29 | 285 | 23.17073 |
| 80000 | 336 | 30.54545 | 297 | 24.14634 |

A13

| Specimen cct25; Normal treated | | | | |
|---|---|---|---|---|
| Crack initiation: $N_i = 44000$; | | | | |
| | meas/a = 10.3 | | meas/a = 13.3 | |
| N | meas | a [mm] | meas | a [mm] |
| 0 | 103 | 10 | 139 | 10.45112 |
| 4000 | 104 | 10.09708 | 153 | 11.50375 |
| 8000 | 105 | 10.19417 | 163 | 12.25563 |
| 12000 | 106 | 10.29126 | 164 | 12.33082 |
| 16000 | 109 | 10.58252 | 175 | 13.15789 |
| 20000 | 113 | 10.97087 | 186 | 13.98496 |
| 24000 | 120 | 11.65048 | 191 | 14.3609 |
| 28000 | 120 | 11.65048 | 197 | 14.81203 |
| 32000 | 120 | 11.65048 | 206 | 15.48872 |
| 36000 | 126 | 12.233 | 213 | 16.01503 |
| 40000 | 136 | 13.20388 | 223 | 16.76691 |
| 44000 | 138 | 13.39805 | 233 | 17.51879 |
| 48000 | 140 | 13.59223 | 243 | 18.27067 |
| 52000 | 140 | 13.59223 | 255 | 19.17293 |
| 56000 | 150 | 14.5631 | 266 | 20 |
| 60000 | 155 | 15.04854 | 281 | 21.12781 |
| 64000 | 155 | 15.04854 | 297 | 22.33082 |
| 68000 | 162 | 15.72815 | 310 | 23.30827 |
| 72000 | 165 | 16.01941 | 328 | 24.66165 |
| 76000 | 175 | 16.99029 | 348 | 26.16541 |
| 80000 | 190 | 18.4466 | 372 | 27.96992 |
| 84000 | 200 | 19.41747 | 399 | 30 |

A14

| Specimen cct26; Normal treated | | | | |
|---|---|---|---|---|
| Crack initiation: $N_i = 46000$; | | | | |
| | meas/a = 7.7 | | meas/a = 8.8 | |
| N | meas | a [mm] | meas | a [mm] |
| 0 | 69 | 8.961038 | 89 | 10.11363 |
| 2000 | 69 | 8.961038 | 89 | 10.11363 |
| 12000 | 71 | 9.220779 | 90 | 10.22727 |
| 22000 | 86 | 11.16883 | 101 | 11.47727 |
| 27000 | 93 | 12.07792 | 105 | 11.93181 |
| 30000 | 96 | 12.46753 | 109 | 12.38636 |
| 33000 | 98 | 12.72727 | 111 | 12.61363 |
| 36000 | 101 | 13.11688 | 115 | 13.06818 |
| 39000 | 103 | 13.37662 | 118 | 13.40909 |
| 42000 | 106 | 13.76623 | 121 | 13.75 |
| 45000 | 108 | 14.02597 | 125 | 14.20454 |
| 48000 | 113 | 14.67532 | 128 | 14.54545 |
| 51000 | 117 | 15.1948 | 134 | 15.22727 |
| 54000 | 122 | 15.84415 | 136 | 15.45454 |
| 57000 | 124 | 16.10389 | 141 | 16.02272 |
| 60000 | 127 | 16.4935 | 145 | 16.47727 |
| 63000 | 133 | 17.27272 | 150 | 17.04545 |
| 66000 | 139 | 18.05194 | 154 | 17.5 |
| 69000 | 142 | 18.44155 | 161 | 18.29545 |
| 72000 | 149 | 19.35064 | 164 | 18.63636 |
| 75000 | 153 | 19.87012 | 172 | 19.54545 |
| 78000 | 159 | 20.64935 | 179 | 20.3409 |
| 81000 | 167 | 21.68831 | 184 | 20.90909 |
| 84000 | 171 | 22.20779 | 191 | 21.70454 |
| 87000 | 180 | 23.37662 | 203 | 23.06818 |
| 90000 | 190 | 24.67532 | 212 | 24.0909 |
| 93000 | 198 | 25.71428 | 220 | 25 |

A15

| Specimen cct27; Cold treated | | | | |
|---|---|---|---|---|
| Crack initiation: $N_i$ = 120000; | | | | |
| | meas/a = 10.5 | | meas/a = 13.1 | |
| N | meas | a [mm] | meas | a [mm] |
| 0 | 131 | 12.47619 | 148 | 11.2977 |
| 8000 | 134 | 12.7619 | 153 | 11.67938 |
| 16000 | 145 | 13.80952 | 158 | 12.06106 |
| 20000 | 148 | 14.09523 | 159 | 12.1374 |
| 24000 | 154 | 14.66666 | 164 | 12.51908 |
| 28000 | 160 | 15.23809 | 169 | 12.90076 |
| 32000 | 162 | 15.42857 | 172 | 13.12977 |
| 36000 | 166 | 15.80952 | 176 | 13.43511 |
| 40000 | 172 | 16.38095 | 180 | 13.74045 |
| 44000 | 179 | 17.04761 | 183 | 13.96946 |
| 48000 | 183 | 17.42857 | 187 | 14.2748 |
| 52000 | 186 | 17.71428 | 193 | 14.73282 |
| 56000 | 192 | 18.28571 | 197 | 15.03816 |
| 60000 | 198 | 18.85714 | 201 | 15.34351 |
| 64000 | 204 | 19.42857 | 208 | 15.87786 |
| 68000 | 211 | 20.09523 | 212 | 16.1832 |
| 72000 | 218 | 20.7619 | 218 | 16.64122 |
| 76000 | 226 | 21.5238 | 224 | 17.09923 |
| 80000 | 234 | 22.28571 | 230 | 17.55725 |
| 84000 | 243 | 23.14285 | 241 | 18.39694 |
| 88000 | 254 | 24.19047 | 249 | 19.00763 |
| 92000 | 264 | 25.14285 | 257 | 19.61832 |
| 96000 | 276 | 26.28571 | 268 | 20.45801 |
| 100000 | 292 | 27.80952 | 280 | 21.37404 |
| 104000 | 313 | 29.80952 | 292 | 22.29007 |

A16

| Specimen cct28; Normal treated | | | | |
|---|---|---|---|---|
| Crack initiation: $N_i$ = 28000; | | | | |
| | meas/a = 10.0 | | meas/a = 13.1 | |
| N | meas | a [mm] | meas | a [mm] |
| 0 | 103 | 10.3 | 147 | 11.22137 |
| 4000 | 108 | 10.8 | 152 | 11.60305 |
| 8000 | 113 | 11.3 | 162 | 12.36641 |
| 12000 | 120 | 12 | 172 | 13.12977 |
| 16000 | 130 | 13 | 178 | 13.58778 |
| 20000 | 138 | 13.8 | 183 | 13.96946 |
| 24000 | 146 | 14.6 | 189 | 14.42748 |
| 28000 | 156 | 15.6 | 201 | 15.34351 |
| 32000 | 166 | 16.6 | 214 | 16.33587 |
| 36000 | 176 | 17.6 | 224 | 17.09923 |
| 40000 | 190 | 19 | 234 | 17.86259 |
| 44000 | 201 | 20.1 | 263 | 20.07633 |
| 48000 | 213 | 21.3 | 278 | 21.22137 |
| 52000 | 230 | 23 | 296 | 22.59541 |
| 56000 | 247 | 24.7 | 319 | 24.35114 |
| 58000 | 256 | 25.6 | 332 | 25.34351 |
| 60000 | 270 | 27 | 344 | 26.25954 |
| 62000 | 288 | 28.8 | 362 | 27.63358 |
| 64000 | 320 | 32 | 387 | 29.54198 |

| Specimen cct29; Cold treated | | | | |
|---|---|---|---|---|
| Crack initiation: $N_i$ = 16000; | | | | |
| | meas/a = 10.0 | | meas/a = 13.1 | |
| N | meas | a [mm] | meas | a [mm] |
| 0 | 98 | 9.8 | 134 | 10.229 |
| 4000 | 100 | 10 | 143 | 10.91603 |

A17

| Specimen cct29; Cold treated | | | | |
|:---:|:---:|:---:|:---:|:---:|
| Crack initiation: $N_i$ = 16000; | | | | |
| | meas/a = 10.0 | | meas/a = 13.1 | |
| N | meas | a [mm] | meas | a [mm] |
| 8000 | 114 | 11.4 | 152 | 11.60305 |
| 12000 | 118 | 11.8 | 162 | 12.36641 |
| 15000 | 123 | 12.3 | 170 | 12.97709 |
| 18000 | 130 | 13 | 179 | 13.66412 |
| 21000 | 137 | 13.7 | 186 | 14.19847 |
| 24000 | 145 | 14.5 | 197 | 15.03817 |
| 27000 | 152 | 15.2 | 207 | 15.80152 |
| 30000 | 159 | 15.9 | 217 | 16.56488 |
| 33000 | 167 | 16.7 | 228 | 17.40458 |
| 36000 | 176 | 17.6 | 240 | 18.32061 |
| 39000 | 187 | 18.7 | 254 | 19.38931 |
| 42000 | 196 | 19.6 | 267 | 20.38167 |
| 45000 | 206 | 20.6 | 281 | 21.45038 |
| 48000 | 216 | 21.6 | 297 | 22.67175 |
| 51000 | 234 | 23.4 | 315 | 24.0458 |
| 54000 | 252 | 25.2 | 337 | 25.72519 |
| 56000 | 265 | 26.5 | 354 | 27.0229 |
| 58000 | 280 | 28 | 376 | 28.70229 |
| 60000 | 310 | 31 | 407 | 31.0687 |

A18